Palacký University Olomouc

Bachelor thesis

Olomouc 2020   Barbora Vrablíková

Palacký University Olomouc

Faculty of Science

Department of Cell Biology and Genetics

Cytotoxicity of microtubule-stabilizing drug laulimalide in hypoxic cancer cell lines

Bachelor thesis

Barbora Vrablíková

Study programme: Biology

Field of study: Molecular and cell biology

Form of study: Full time

Olomouc 2020   **Supervisor: Mgr. Viswanath Das, Ph.D.**

BIBLIOGRAPHICAL IDENTIFICATION

Author's name   Barbora Vrablíková

Title   Cytotoxicity of microtubule-stabilizing drug laulimalide in hypoxic cancer cell lines

Type of thesis   Bachelor

Department   Cell Biology and Genetics, Faculty of Science UP, Olomouc

Supervisor   Mgr. Viswanath Das, Ph.D.

The year of defense   2020

Summary

Microtubule stabilizing agents are extensively used in the anticancer treatment of solid tumours. Their effect consists of promoting the polymerization of microtubules, thereby stabilizing them and disrupting the function of the mitotic spindle, which leads to cell apoptosis. Paclitaxel, a microtubule-stabilizing drug widely used in chemotherapy, struggles with hypoxia-induced resistance, so there are being sought alternatives without the hypoxia-limited effect. Laulimalide is another microtubule-stabilizing drug, with a different binding site on the tubulin dimer than paclitaxel. Its ability to inhibit cell viability in a hypoxic environment was confirmed in this work by repeated cytotoxicity assays in hypoxic cancer cell lines. Using the *in vitro* tubulin polymerization assay was also confirmed the ability of laulimalide to induce tubulin polymerization.

Keywords   anticancer drugs, MSA, laulimalide, hypoxia, cytotoxicity

Number of pages   49

Number of appendices   0

Language   English

BIBLIOGRAFICKÉ ÚDAJE

Souhrn

Látky stabilizující mikrotubuly jsou hojně využívány se v léčbě solidních nádorů. Jejich efekt spočívá v indukci polymerizace mikrotubulů, tímto dochází k jejich stabilizaci a narušení funkce dělícího vřeténka, což vede k buněčné smrti. Paklitaxel, široce využívaná látka v chemoterapii stabilizující mikrotubuly, se potýká s rezistencí indukovanou hypoxií, proto jsou hledány alternativy, které by byly schopny se tomuto léku účinkem vyrovnat, přičemž by nebyly právě hypoxií limitovány. Laulimalid je další látkou stabilizující mikrotubuly, avšak s rozdílným vazebným místem na tubulinovém dimeru. Jeho schopnost inhibovat buněčnou viabilitu v hypoxickém prostředí byla v této práci potvrzena opakovanými testy cytotoxicity v hypoxických nádorových liniích. Pomocí testu polymerizace tubulinu *in vitro* byla v těchto buňkách také potvrzena schopnost laulimalidu indukovat tubulinovou polymerizaci.

DECLARATION

I declare, that this bachelor thesis was written independently with the help of my supervisor Mgr. Viswanath Das, Ph.D., and using the sources listed in the references.

In Olomouc, ………………………   ………………………………

                                                                    Barbora Vrablíková

ACKNOWLEDGMENT

CONTENT

ABBREVIATIONS

A549	Human alveolar epithelial adenocarcinoma cell line
ATP	Adenosine triphosphate
CA4	Combretastatin A4
DDM	Discodermolide
DTX	Docetaxel
EB1	End-binding protein 1
Epo	Epothilones
GDP	Guanosine diphosphate
GTP	Guanosine triphosphate
HCT116	Human colorectal carcinoma cell line
HIF	Hypoxia-inducible factor
IC$_{50}$	Half-maximal inhibitory concentration
LAU	Laulimalide
MAP	Microtubule-associated protein
MDA	Microtubule-destabilizing agent
MDR	Multidrug resistance
MSA	Microtubule-stabilizing agent
MT	Microtubule
MTA	Microtubule-targeting agent
MTD	Microtubule-targeting drugs
MTOC	Microtubule-organizing centre
MTT	3-[4,5-dimethylthiazol-2-yl]-2,5-diphenyltetrazolium bromide
P-gp	P-glycoprotein
PHD	Prolyl hydroxylase domain
PLA	Peloruside A
PMSF	Phenylmethylsulphonyl fluoride
PTX	Paclitaxel
SDS	Sodium dodecyl sulphate
TME	Tumour microenvironment
TUBB3	Tubulin beta 3 class III

LIST OF FIGURES

LIST OF TABLES

1   INTRODUCTION

Microtubules are an essential element in chemotherapy. For many anti-cancer drugs, microtubules are a target and the disruption of their dynamic behaviour is a key to inhibit tumour growth. However, the treatment itself complicates the hypoxic environment of tumours, which is responsible for the lower sensitivity of cancer cells to chemotherapy. The result of hypoxic conditions effects on cancer cells includes changes in tubulin conformation, altered expression of tubulin isotypes, and metabolic pathways. Paclitaxel is a taxane that has been extensively used in chemotherapy for many years to treat various types of cancer, such as breast, cervical, lung cancer, and Kaposi sarcoma, however, the treatment also struggles with hypoxia-induced resistance. Therefore, various alternatives with similar effects as paclitaxel are being sought, without the limitation of hypoxia.

Recent cellular studies have shown that peloruside A, a microtubule-stabilizing agent (MSA) similar to paclitaxel, is more effective in hypoxic cancer cells than paclitaxel potentially due to a different microtubule-binding site that is not significantly affected by hypoxic conditions as the taxane-binding site. Laulimalide, similar to peloruside A, is a non-taxane MSA and both of these MSAs have the same microtubule-binding domain and potentially better cytotoxic effect in cancer cells affected by hypoxia. This thesis is focused on testing the cytotoxicity of laulimalide and compare that to paclitaxel in normoxic and hypoxic environments and determine the ability of laulimalide to stimulate microtubule assembly and tubulin polymerization in hypoxia.

2 AIMS OF THE THESIS

The first aim of this thesis was to determine the effects of laulimalide on selected cancer cell lines – HCT116 and A549 under hypoxic conditions and compare that to normoxic conditions. Microtubule-stabilizing drugs such as paclitaxel or docetaxel used in cancer treatment are often prone to hypoxia-mediated resistance. Therefore, it is important to find alternative MSAs that result in similar cell responses in hypoxic conditions as in normoxia. Laulimalide binds to a different site of the microtubule than taxanes. Since hypoxia is known to reduce the response of cancer cells to taxanes, we hypothesized that non-taxane MSA, laulimalide, would have better cytotoxicity on hypoxic cancer cells.

The second aim of this thesis was to determine the effects of laulimalide on tubulin polymerization in hypoxic conditions following the treatment with drugs to confirm its microtubule-polymerizing effects.

3 LITERATURE REVIEW

3.1 Microtubules

Microtubules are 25-nm diameter hollow cylindrical cytoskeletal structures with variable length and composed of repeating subunits α-tubulin and β-tubulin, which are assembled around a central empty core (Alberts *et al.*, 1994). Every microtubule cylinder of polymerized heterodimers is formed by 13 protofilaments oriented in a parallel way with the same polarity such as the plus (+) end of microtubule ends with a β–tubulin subunit and minus (–) end ends with a α-tubulin subunit. These protofilaments form a sheet-like structure and bind to γ-tubulin, another member of the tubulin family, which is located in the microtubule-organizing centre, the place where new microtubules are formed. The information about assembly of dimers to protofilaments is encoded in the tubulin sequence (Nogales, 2001). The ability of microtubules to switch between shrinking (depolymerize) and growing (polymerize) states is aided by guanosine-5'-triphosphate (GTP), and this process is described as dynamic instability (Alberts *et. al*, 1994; Nogales, 2001). Microtubules maintain a lot of different functions in a cell, however, their dynamic behaviour is based on which role they hold (Avila, 1991). Disruption of microtubule's dynamic instability is targeted in cancer therapy, whether by stabilizing the tubulin polymerization or inducing tubulin depolymerization (Alberts *et. al*, 1994).
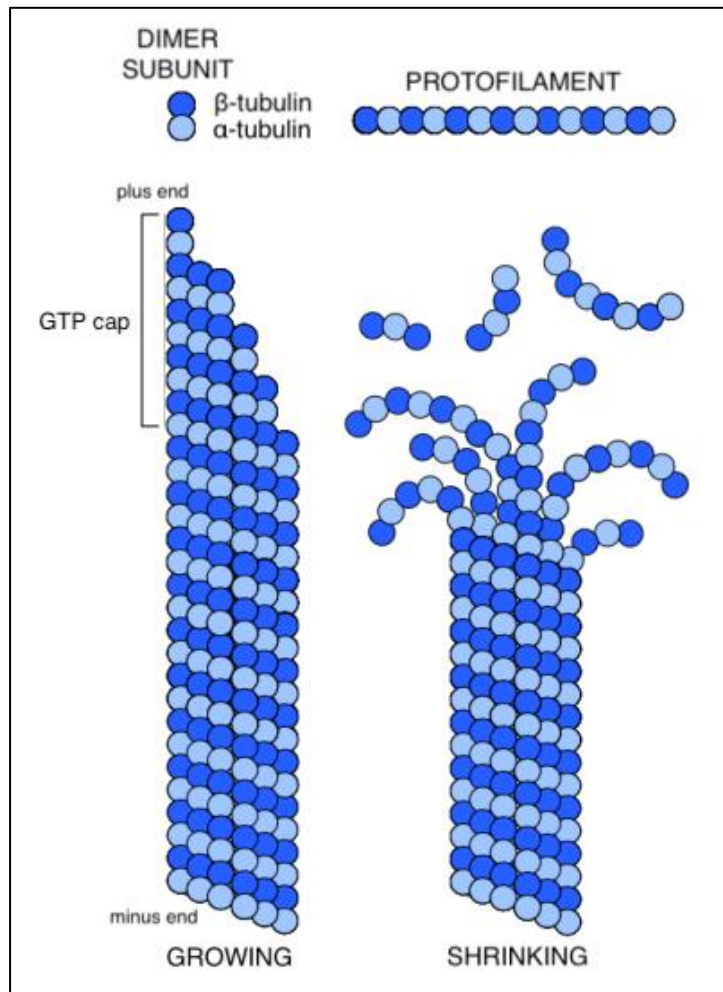
Figure 3.1 Microtubules are composed of α- and β-tubulin subunits that come together to first form a heterodimer and then protofilaments that result in their polarity (plus and minus end). The growing (polymerization) and shrinking (depolymerization) on the plus end of a microtubule is shown. Adjusted according to Alberts *et al*., 2002

3.1.1 α- and β-tubulin

The structure of both types of tubulin is identical – tubulin molecule is made up of two β-sheets located in the central part of molecule formed by ten β-strands, which are surrounded by twelve α-helices. This structure is divided into N-terminal (GTPase domain), central and C-terminal domain. The N-terminal domain comprises GTP and GDP binding sites, the central domain has a paclitaxel-binding site located on the outer surface that interacts with microtubule-associated proteins (MAPs). The N-terminal domain includes six α-helices (H1–H4) and five β-strands (B1–B5), the central domain is formed out of four α-helices (H7–H10) and four β-strands (B7–B10) and the C-terminal domain includes two α-helices (H11 and H12). Microtubules interact with nucleotides of binding partners via α-helices H7 and H8 in the central domain. Lateral tubulin contacts are mediated by M-loop, located between α-helix H9 and β-strand H3, and loop between α-helix H1 – β-strand B2 and α-helix H3 (Nogales *et al.*, 1998).

3.1.2 Dynamic instability

The dynamic instability of microtubules is referred to as the dynamic switch between polymerization (growing) and depolymerization (shrinking), which is based on GTP binding and hydrolysis. There are two nucleotide sites on microtubules where GTP molecules bind to tubulin monomer: the exchangeable E-site on β-tubulin and nonexchangeable N-site on α-tubulin. This binding is in stoichiometric equilibrium, that is, one molecule of GTP binds to one molecule of tubulin. The binding of GTP to E-site usually takes place after the polymerization and with the hydrolysis of GTP to GDP (Nogales, 2001). The dynamic imbalance behaviour of microtubules is critical for their standard function and is caused by slow hydrolysis of GTP followed by tubulin polymerization. The hypothesis of the GTP cap model explains that microtubules formed by GDP-tubulin subunits are not stable because of their low-affinity binding, however, the microtubule stabilization is ensured by the GTP-tubulin layer – the GTP cap. Without the GTP cap, the GDP-tubulin subunits are exposed, microtubules lose the stability and rapidly depolymerizes, this process is called a catastrophe. The reverse process that results in shrinkage to growth is called microtubule rescue (Alberts *et al.*, 1994; Nogales, 2001). When the microtubules disassemble, protofilaments curves and forms rings (Amos, 2011).

The GTP on the N-site of α-tubulin is not hydrolysed, the binding site for GTP is inaccessible on α-tubulin unlike the GTP binding site on β-tubulin (Nogales *et al.*, 1998). The hydrolysis of GTP enables microtubules to depolymerize by weakening tubulin subunits and the binding of GTP to tubulin is important for microtubules to polymerize. The positive end of the microtubule is a fast-growing end and is oriented to the outside of the microtubule-nucleating site – centrosomes that are poles of the mitotic spindle or basal body of the cilium, whereas the negative end is slow-growing. The centrosomes form organizing centre of microtubules (MTOC), which is an initiation site for microtubule assemble, located on one side of the nucleus during the interphase stage of the cell cycle. Blockage of microtubule polymerization for example by colcemid can be noted at this place (Bornens, 2012). During the interphase, the centromere is divided into two identical parts, which later form the mitotic poles of the mitotic spindle during mitosis (Alberts *et al.*, 1994). The MTOC differs between different cell types. In mammalian and lower plants, microtubules are organized around centrosomes, whereas in higher plants the centrosomes are absent (Lambert, 1993; Vaughn, 2013). In the cell cycle of higher plants, there are five arrays formed by microtubules and actin filaments – the cortical and the radial cytoplasmic arrays, the preprophase band, the mitotic spindle and the phragmoplast (Lambert, 1993). The centrioles are absent in mouse oocytes, in fungi and diatoms, they are present as spindle pole bodies. Nevertheless, all MTOC, irrespective of the type of living species, contain specific centriole proteins, such as γ-tubulin responsible for nucleation and already mentioned α- and β-tubulin (Alberts *et al.*, 1994).
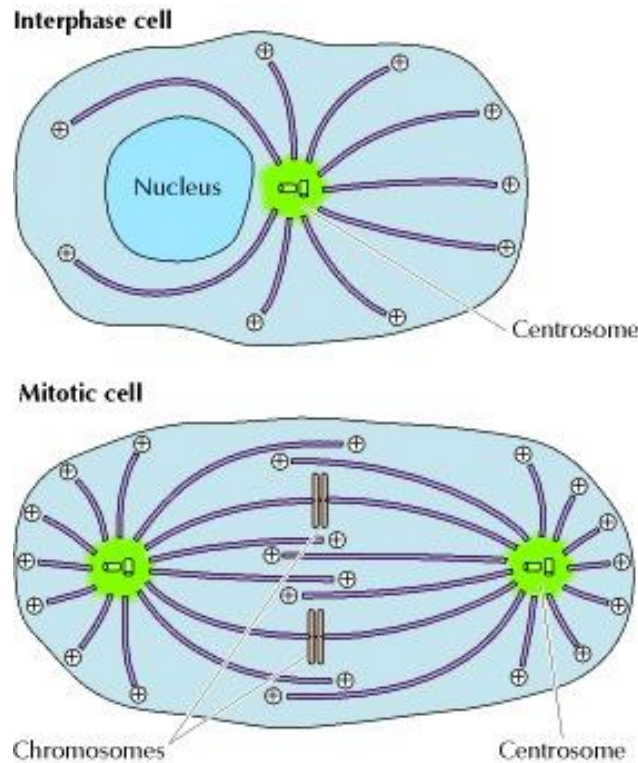
Figure 3.2 The scheme of interphase and mitotic cells. In the interphase cells, there is one centrosome located nearby the nucleus and in a mitotic cell, the centrosome is duplicated. The positive end of a microtubule is located outside of centrosome, whereas the negative end is anchored in the centrosome (Cooper, 2000).

3.1.3 Microtubule function

In general, microtubules are an indispensable component affecting cell transport, motility, division, and also shape. Microtubule functions differ between the microtubule populations, and the role is based on the ability of tubulin polymerization (Avila, 1991). Microtubules are important cytoskeletal components together with intermediate filament and microfilaments, which are present in eukaryotic cells and play an important role in their spatial organization. In animal cells, microtubules are organized in radial arrays called asters, and during the cell division, asters can quickly rearrange themselves into the mitotic spindle. In the interphase of cell division, microtubules are responsible for the intracellular organization. In animal cells, microtubules radiate from the centrosome and grow or shrink because of their dynamic instability. The loss of depolymerized microtubules is balanced by the polymerizing of other ones (Alberts *et al.*, 2002). During prophase/prometaphase, microtubules self-assemble in the cytoplasm, form a mitotic spindle, and bind to kinetochores, the protein structure near the centromere of chromosomes. In metaphase, they are involved in the arrangement

of chromosomes into the metaphase plate, the dynamic instability of microtubules increase during this phase. The shortening of microtubules causes separation of chromosomes and distribution to daughter cells (Jordan *et* Wilson, 2004).

Another function of microtubules is to secure the positions of organelles located close to the membrane and participates in cell transport. Besides, microtubules are important constituents of axonemes in cilia and flagella located on the cell surface and involved in cell movement or occur as microtubule bundles in axon and dendrites located in neurons. Their function differs according to dynamic activity and MAP proteins (Alberts *et al.*, 2002; Avila, 1991). Microtubules play an important role in morphological types of cells together with different MAPs, for example in the nervous system, uniformly oriented microtubules of axon comprise tau proteins and differently oriented dendrites MAP2 proteins. The orientation of microtubules and association with different MAPs is crucial in axonal transport (Avila, 1991).

Table 3.1 Different microtubule structure and their functions (Avila, 1991).

Structure	Function	Increased stability
Mitotic spindle	Chromosome segregation	
Interphase MT network	Intracellular organization	
Dendrites	Neural morphogenesis, postsynaptic densities	
Axon	Neural morphogenesis, presynaptic densities, axonal transport	
Cilia, flagella	Cell motility	
Basal bodies, centrioles		
Axonemes		

3.1.4 Tubulin post-translational modifications and MAPs

Tubulin subunits, which form microtubules, contain in their structure and sequence information about assembling and can be modified after tubulin polymerization via posttranslational modification of their negatively charged C-terminal end, such as acetylation, tyrosination, phosphorylation or polyglutamylation (Nogales, 2001).

The acetylation of α-tubulin on specific lysine is the slowest process among all posttranslational modifications. These modifications can help determine the time when the microtubules were polymerized (Alberts *et al.*, 1994). In mammalian cells, there are multiple α- and β-tubulin isotypes, each one encoded by a different gene (Alberts *et al.*, 1994). Divergency of these isotypes in dynamic behaviour correlates with resistance in cancer treatment (Nogales, 2001).

The individual microtubule functions are also based on interactions of their negatively charged C-terminal ends with positively charged microtubule-associated proteins (MAPs), which affect the expression of microtubules (Nogales, 2001; Jordan *et* Wilson, 2004). There are different types of MAPs responsible for microtubule distribution and stabilization in cells, such as motor proteins, dynein and kinesin, tau, stathmin, MAP1, MAP2, MAP4, and others. Kinesin and dynein are two well-known microtubule-dependent motor proteins. Kinesin-dependent proteins move towards the plus-end of microtubules, conversely, dynein-dependent proteins move towards the minus-end of microtubules. Some of the MAPs are closely associated with resistance of anti-cancer drugs, (Alberts *et al.*, 2002; Jordan *et* Wilson, 2004; Nogales, 2001). For example, tau protein, with microtubule-stabilizing role, negatively affects PTX treatment in breast cancer. Conversely, high expression of MAP2 with the same role in microtubule dynamics as tau protein, has positive effects on anticancer treatment with PTX. Also, EB1 protein, which supports microtubule polymerization and its stabilization is a regulator of PTX responsiveness. Low expression of microtubule-destabilizing protein stathmin has been confirmed as positive in PTX treatment, as much as with survivin (Xie *et al.*, 2015). To improve stabilization of microtubules in neurons, under the influence of cold temperature or destabilizing agents, the MAPs include calmodulin-regulated protein which is responsible for the stabilization (Nogales, 2011).

3.1.5 Microtubule-Targeting drugs

Microtubules are very labile and sensitive to chemical agents that affect their function. Their crucial role in cell division forms a major basis in cancer treatment. The process of microtubule shrinking or growing can be easily disrupted by tubulin-binding drugs, which leads to anomalous microtubule behaviour (Nogales, 2001). Microtubule-targeting agents (MTAs), affecting microtubule functions, are most

likely natural molecules produced by plants or marine sponges (Jordan *et* Wilson, 2004). MTD can be classified into two categories – microtubule-destabilizing agents (MDAs), which inhibits tubulin assembling inhibiting mitotic spindle formation, and microtubule-stabilizing agents (MSAs), which prevent the depolymerization of microtubules (Amos, 2011). For example, colchicine, an alkaloid extracted from the autumn crocus (*Colchicum autumnale*) founded in 1968 (Field *et al.*, 2014) binds to tubulin molecule and thereby inhibiting tubulin polymerization. If the microtubule is formed – tubulin is already polymerized, in such a condition, colchicine is unable to bind to tubulin. Other examples of MDAs are vincristine, vinblastine, 2-methoxyestradiol, combretastatin, and others (Alberts *et al.*, 1994; Field *et al.*, 2014; Jordan *et* Wilson, 2004). MSAs, such as paclitaxel, docetaxel, epothilones, laulimalide, and cematodin stabilize the microtubules and assemble unbound tubulin molecules to microtubules, thereby preventing their depolymerization during the cell division (Alberts *et al.*, 1994; Jordan *et* Wilson, 2004; Nogales, 2001).

3.2   Microtubule-Destabilizing Agents

The anti-proliferative activity of MDAs is based on their ability to inhibit the assembly of tubulin. Disassembly of microtubules leads to the creation of small rings or tubulin protofilaments, which transform into long spirals. In examples of MDA class of anti-mitotic drugs belong molecules with two different binding sites on microtubule which destabilize them – binding within the heterodimer (colchicine domain binding site) and binding between heterodimers (Vinca domain binding site) (Amos, 2011).

Vincristine, vindesine, vinorelbine, and vinblastine are three examples of Vinca alkaloids with the Vinca domain binding site, which are widely used in the clinic cancer therapy. For example, vinblastine is used for lymphomas, breast, and bladder cancer treatment. These substances were isolated from pink periwinkle *Catharantus roseus* leaves, which were used in medicine since the 17th century. The first use of Vinca alkaloids due to their antimitotic properties was in the 1950s for the treatment of hematologic malignancies. The binding site of Vinca alkaloids is located on β-tubulin of soluble tubulin heterodimer, and this binding causes conformational changes of tubulin. The main effect of Vinca MDAs results from the inhibition of the mitotic spindle formation following depolymerization of microtubules, which

causes

the blocking of cells with condensed chromosomes in mitosis. These effects occur at higher concentrations of Vinca alkaloid (10–100 nmol·l^{-1}). Dynamic instability results when Vinca alkaloid molecules bind to microtubule plus ends. However, Vinca alkaloids are known to have significant side effects such as peripheral neuropathy, suppression of bone marrow activity, constipation, nervous system toxicity, and nausea (Jordan *et al.*, 2004).

Another Vinca domain binding agent is Halichondrin B, polyether macrolide, obtained from sponge *Halichondrin okadai*. However, because of the low yields, it was focused to synthesize derivates, such as eribulin, with a different binding site and effects on tubulin. Eribulin is FDA approved drugs used in breast cancer treatment and other malignancies (Amos, 2011; Bates *et al*., 2017). Other examples of drugs with Vinca-binding site can be alkaloid Rhazilinam, Dolastation-10 isolated from mollusc *Dolabella auricularia* or tripeptide Hemiasterlin isolated from sponge *Miasterella minor* and other (Amos, 2011).

In the group of MDAs with colchicine binding site belongs Combretastatin A4 (CA4), isolated from bush willow *Combretum caffrum*. CA4 is known as a strongly potent drug and results in metastasis blocking by inhibition of tumour vasculature. The clinical trials have shown serious side effects such as neurotoxicity, heart damage, and thromboembolic diseases (Bates *et al*., 2017). Also, 2-methoxyestradiol belongs to the group of MDAs which binds to the colchicine domain. The inhibitory effects on a metastatic breast cancer made this drug a potential candidate in the treatment, but the neurotoxicity and poor efficacy avert further clinical trials (Rahman *et al*., 2018). Nocodazole, another colchicine-binding site agent, is a toxin isolated from *Podophyllum peltatum* Podophyllotoxin blocks cell in mitosis and has antitumour activity (Amos, 2011).

3.3   Microtubule-Stabilizing Agents

MSAs are a group of drugs that induce the assembly and inhibition of depolymerization of microtubules (Alberts *et al.*, 1994; Nogales, 2001). MSAs, such as paclitaxel, docetaxel, epothilones, and discodermolides are an important class of anticancer drugs that are currently used in the clinic for cancer therapy or are in various phases of clinical trials. Most often they are derived from natural products. MSA-treated cells fail to pass the mitotic checkpoints that cause cell death

11

(Jordan *et* Wilson, 2004). MSAs are highly cytotoxic and cause a change in microtubule dynamics even at a very low nanomolar concentration (Altmann, 2001).

3.3.1 Paclitaxel and docetaxel

Paclitaxel (Taxol®), discovered in 1992 from the bark of yew trees *Taxus brevifolia* (Amos, 2011), is a diterpenoid and belongs to taxanes class of MSAs (Altmann *et al*., 2000). PTX is extensively used in the treatment of different solid tumour types, such as breasts, ovaries, lung, and Kaposi's sarcoma alone or in combination with its semisynthetic analogue, docetaxel (Jordan *et* Wilson, 2004). The cell after treatment with PTX is unable to pass the G_1 or M-phase of mitosis and eventually die or escape by mitosis slippage (Arnal *et al*., 1995). The binding site of PTX is located at the luminal side of β-tubulin subunit. This binding pocket is formed by the S9-S10 loop and H1, H6, and H7 helices parts (Nogales *et al*., 1998). The most important part of PTX, the taxane ring, interacts with M-loop and stabilizes the microtubules. The stoichiometry of PTX molecules to the binding site in tubulin is 1:1, which means that one molecule of tubulin has one PTX binding site. Microtubules in PTX-treated cells start to assemble and form bundles due to conformational changes in tubulin that increase the affinity of tubulin molecules for each other (Jordan *et* Wilson, 2004). The tubulin depolarization is blocked even under the influence of Ca^{2+} or cold (4 °C) (Schiff *et al*., 1979).

Unfortunately, the use of PTX and DTX in chemotherapy is limited by their dose-dependent side effects such as neurotoxicity, myelosuppression, alopecia, and hypersensitivity reactions (Bollag *et al*., 1995; Jordan *et* Wilson, 2004). Further, both PTX and DTX are a good substrate for the P-glycoprotein efflux pump, which is an obstacle in cancer treatment (Bollag *et al*., 1995).

3.3.2 Epothilones

Fungicidal macrolides epothilones were first discovered in 1995 (Altmann *et al*., 2000) as a metabolite from *Sorangium cellulosum* with similar mechanisms of microtubule stabilization to PTX. Epothilones induce microtubule assembly and formation of multipolar spindles, microtubule bundling and mitotic arrest. Synthetic analogues of epothilones, such as epothilone A and epothilone B have different

cytotoxicity. Whereas EpoB is more cytotoxic than PTX, the cytotoxicity of EpoA is similar to PTX (Altmann *et al*., 2000). The binding site of epothilones on tubulin is similar to PTX, and therefore, epothilones antagonists' effect due to higher affinity for microtubule binding when combined with paclitaxel (Bollag *et al*., 1995; Goodin *et al*., 2004). Interestingly, despite the similar microtubule binding site and mechanism of microtubule stabilization, the epothilones are less susceptible to efflux by P-glycoprotein than PTX (Goodin *et al*., 2004). Mutations in β-tubulin reduces their activity similar to paclitaxel (Altmann, 2001). Epothilones can prevent the disassembly of microtubules promoted by Ca^{2+} or cold *in vitro* and also support microtubule polymerization even if the GAP cap is not present. Another advantage of epothilones over paclitaxel is their ability to inhibit the growth of multidrug-resistant cancer cells (Altmann *et al*., 2000).
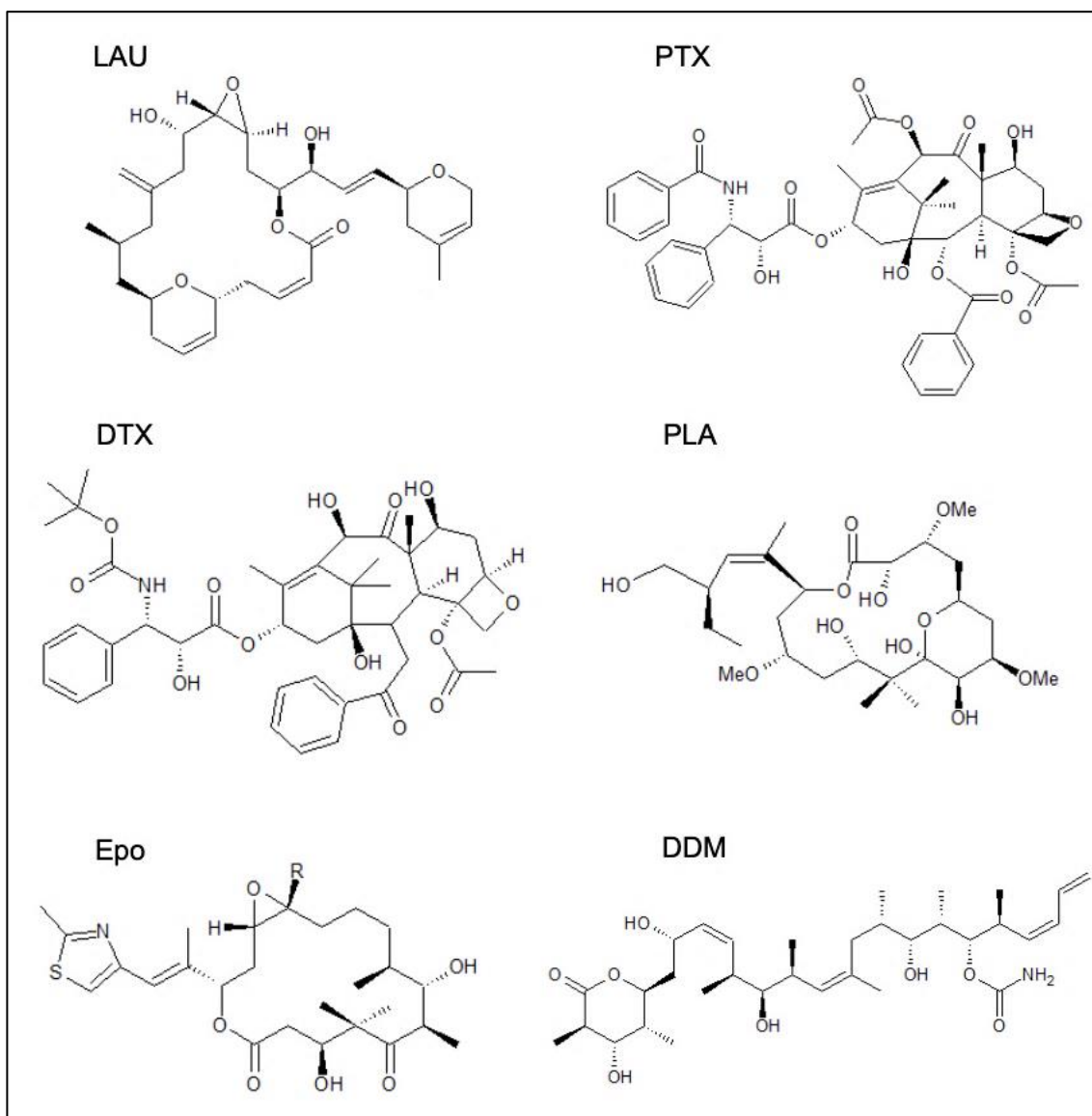
3.3.3 Laulimalide and Peloruside A

LAU is a cytotoxic MSA isolated from marine sponge *Cacospongia mycofijiensis*. Marine organisms are a rich source of microtubule-targeting products, therefore different marine extracts are extensively tested for their use as antimitotic agents, including PLA isolated from *Mycale hentscheli* sponge (Amos, 2011). The binding site of LAU and PLA is located on β-tubulin differing from the taxane binding site (Kanakkanthara *et al*., 2011). An X-ray crystallography study has shown that the binding site of LAU a PLA is formed by helices H9 and H10 and loops H9-H9 and H10-S9, whereas these agents also interact with M-loop (Kanakkanthara *et al*., 2015). LAU and PLA have shown significant anti-cancer properties due to their paclitaxel-like microtubule-stabilizing activity. Since PLA and LAU bind to a different site on β-tubulin than PTX, they show improved activity by blocking cells in G2 and M phases of the cell cycle and inducing apoptosis in cells that are resistant to PTX and epothilones (Moobery *et al*., 1999; Kanakkanthara *et al*., 2011). The exposure of LAU or PLA-treated microtubules to cold or $CaCl_2$ does not cause microtubule depolymerization, suggesting their strong association with tubulin (Moobery *et al.*, 1999). Compared to PTX, PLA and LAU are a poor substrate of the P-glycoprotein efflux pump (Kanakkanthara *et al*., 2011). Efficacy of LAU has been confirmed in human ovarian cancer cell lines SKOV-3 (Altmann, 2001) and PLA is a potential candidate for the treatment of neurological and immune diseases (Kanakkanthara *et al*., 2015).

3.3.4 Discodermolide

Discodermolide, a polyketide, is another MSA isolated from marine sponge *Discodermia dissolute* with stronger antimitotic activity than PTX (Amos, 2011), but also with immunosuppressive activity (Hearn *et al*., 2007). DDM is a poor substrate for Pg-pump as Epo and studies have shown, that DDM is an effective inhibitor of cell proliferation in taxol-resistant cancer cell lines. The combination of DDM and PTX used in carcinoma treatment exhibits synergy in their action, whereas this synergistic relationship is not fully understood (Gertsch *et al*., 2009; Jordan *et* Wilson, 2004). Clinical trials of DDM have been stopped after the discovery of serious side effects such as interstitial pneumonitis (Hearn *et al*., 2007).

Figure 3.3 Chemical structures of laulimalide (LAU), paclitaxel (PTX), docetaxel (DTX), peloruside A (PLA), epothilone (Epo), discodermolide (DDM)

3.4 Resistance to antimitotic drugs

Resistance to anti-mitotic drugs is a major hurdle in the treatment of many cancer types and arises due to various factors. The first problem is associated with overexpression of transporter proteins – ATP-dependent drug efflux pumps. Low levels of intracellular accumulation of drugs due to efflux pumps lead to multidrug resistance (MDR) to different antimitotic drugs. The most common is the P-gp efflux pump, a product of the MDR1 gene (Jordan *et* Wilson, 2004). Also, expression of different tubulin isotypes and their conformational changes, together with the upregulation of MAPs (for example MAP-4 and tau) (Goodin *et al*., 2004), abnormal expression of miRNA and altered apoptotic pathways (Kanakkanthara *et al*., 2011) are other factors that contribute to resistance to anti-mitotic anti-cancer agents

3.5 Hypoxia in solid tumours

Tumour hypoxia is a significant obstacle in cancer treatment. Poor diffusion of oxygen into inner regions of tumours results in defective vasculature which leads to this hypoxic condition. The hypoxic environment affects the characteristics of both malignant and non-malignant stromal cells in the tumour microenvironment (TME). These changes in both the cell types of the TME alter tumour cell response to chemotherapy or radiotherapy (Höckel *et* Vaupel, 2001). Hypoxia alters tubulin conformation and microtubule stability, thereby altering the response of cells to certain MTAs (Das *et al*., 2015). Further, the oxygen level in solid tumours influence their growth, malignant potential and tumour cell spread in the vicinity of the tumour but also in the whole body because of genome instability and clonal selection (Höckel *et* Vaupel, 2001; Vaupel *et al*., 2001). Hypoxia levels within the tumours differ and can be categorized from mild hypoxia (≤ 2 % O_2) to severe hypoxia (< 0.1 % O_2) (Takáčová *et* Pastoreková, 2015). Hypoxic environment causes a deficiency of not only oxygen but also ATP, which leads to a failure in the Na^+ and K^+ gradient, increased levels of cytosolic Ca^{2+}, membranes depolarization, cell swelling, or tumour acidosis due to a decrease of the cytosolic pH (Höckel *et* Vaupel, 2001).

3.5.1 Factors resulting in hypoxia

The poor oxygen level or even absence of oxygen supply to tumour cells is a result of morphological changes in the microvasculature that affects tumour microcirculation. Compared to affected regions, hypoxic regions have significantly less O_2 tension. Several

key factors result in tumour hypoxia, such as transient perfusion-limited hypoxia or diffusion-limited hypoxia, which is chronic hypoxia caused by insufficient oxygen supply. Tumour or therapy-induced hypoxia is associated with reduced ability of blood to transfer O_2, a problem that persists in toxic hypoxia when blood has a higher affinity to carry CO than O_2, resulting in the formation of the carboxyhaemoglobin (HbCO) (Vaupel *et al*., 2001).

Table 3.2 Hypoxia causing factors (Vaupel *et al*., 2001)

Perfusion-limited hypoxia	Abnormal microvessels structure
	Abnormal microvessels function
	Transient flow stasis (ischemia)
Hypoxia caused by anaemia	Anaemia associated with tumour
	Anaemia induced by therapy
Hypoxemic hypoxia	Plasma flow only
	Micro vessels arising from the venous side
Diffusion-limited hypoxia "chronic hypoxia"	Enlarged diffusion distances
	Adverse diffusion geometry
Toxic hypoxia	HbCO formation (in heavy smokers)

3.5.2 Tumour hypoxia and hypoxia-inducible factor-1

Hypoxia-inducible factor-1 (HIF-1) is a key transcriptional factor of hypoxia and mediator of hypoxic responses to anticancer drug resistance. HIF-1 is a heterodimer composed of oxygen-sensitive HIF-1α present at low concentrations and constitutively expressed HIF-1β. Under low oxygen concentration, dimerization of α- and β-subunits result in the key transcription of key hypoxia-associated factors (Vaupel *et al*., 2001). Cells can survive in a low oxygen environment by reducing their metabolic activities, which is resulted by HIF-1α subunit (Das *et al*., 2015). The HIF-1α-/β heterodimer functions as a hypoxic transcription factor by binding to the hypoxia response element (HRE) and regulating gene expression. As a result, a multitude of genes are activated, such as glucose transporters, vascular endothelial growth factor, genes associated

with Bcl-2 family responsible for apoptosis, epidermal growth factor (Vaupel *et al*., 2001). Under normoxia, HIF-1α is maintained at a low concentration by their degradation through the prolyl hydroxylase domain (PHD) and the proteasome. Compared to HIF-1 negative patients, HIF-1-positive patients live shortly up to five years less (Das *et al.*, 2015).

HIF-1α is expressed in 50 % of solid tumours, however, it was confirmed that DTX is capable of downregulating HIF-1 levels and retain cytotoxicity in hypoxic prostate cancer cells. Resistance to different MTD is associated with overexpression or suppression of pathways that are altered by hypoxia, for example, inhibition of glycogen synthase kinase-3 in MDA-MB-231 cells (breast cancer) causes resistance to vincristine or vinblastine, whereas, overexpression of TUBB3 is associated with resistance to PTX and DTX (Das *et al*., 2015).

4 MATERIALS AND METHODS

4.1 Chemicals and reagents

- o $10\times$ Tris Buffered Saline (TBS) (Bio-Rad, cat. No. 1706435)
- o $10\times$ Tris/Glycine/SDS electrophoresis buffer (Bio-Rad, cat. No. 1610772)
- o 30% Acrylamide/Bis-acrylamide (Bio-Rad, cat. No. 1610156)
- o 7.5% Sodium bicarbonate (Gibco™, cat. No. 25080094)
- o 98% Ethanol (Sigma-Aldrich)
- o alamarBlue™ Cell Viability Reagent (ThermoFisher Scientific™, cat. No. DAL1025)
- o Alexa Fluor 488 conjugated goat anti-mouse IgG secondary antibody (ThermoFisher Scientific™, cat. No. A-21202)
- o Alpha-Tubulin (α-Tubulin) mouse monoclonal antibody (ThermoFisher Scientific™, cat. No. T5168)
- o Bovine serum albumin (BSA) (Sigma-Aldrich, cat. No. A2153)
- o Fetal bovine serum (FBS) (Gibco™, cat. No. 10270106)
- o Protease Inhibitor Cocktail Tablets (Roche, cat. No. 04693116001)
- o Resolving gel buffer 1.5 M Tris-HCl; pH 8.8 (Bio-Rad, cat. No. 161-0789)
- o Spectra™ Multicolor Broad Range Protein Ladder (ThermoFisher Scientific™, cat. No. 26634)
- o Stacking gel buffer 0.5 M Tris-HCl; pH 6.8 (Bio-Rad, cat. No. 161-0799)
- o Tetramethylethylenediamine (TEMED) (Bio-Rad, cat. No. 1610801)
- o Thiazolyl Blue Tetrazolium Bromide (MTT) (Sigma-Aldrich, cat. No. M2128)
- o TrypLE™ Express Enzyme $1\times$, no phenol red (ThermoFisher Scientific™, cat. No. 12604013)
- o β-Mercaptoethanol (Sigma-Aldrich, cat. No. M6250)

4.2 List of solutions

- 10× PBS: 80 g NaCl, 2.0 g KCl, 14.4 g Na_2HPO_4, 2.4 g KH_2PO_4 dissolved in 800 ml dH_2O, pH adjusted to 7.4 with HCl and added dH_2O to 1000 ml, sterilized by autoclaving

- 10% (w/v) APS: 0.10 g of APS dissolved in 1 ml of dH_2O

- 10% (w/v) SDS: 1 g of SDS dissolved in 10 ml of dH_2O

- 12% resolving polyacrylamide gel: 4 ml 30% acrylamide/bis-acrylamide, 3.2 ml dH_2O, 2.6 ml resolving gel buffer, 100 µl 10% (w/v) SDS, 100 µl 10% (w/v) APS, 10 µl TEMED

- 5× SDS-PAGE loading buffer: 250 $mmol \cdot l^{-1}$ Tris-HCl (pH 6.8), 10% SDS, 30% (w/v) glycerol, 0.5 $mol \cdot l^{-1}$ DTT, 0.02% (w/v) Bromphenol Blue, 10% Mercaptoethanol

- 5% (w/v) BSA blocking solution: 2 g of BSA dissolved in 30 ml of TBST buffer, added TBST to 40 ml

- Hypotonic lysis buffer: 157.6 mg Tris-HCl (10 $mmol \cdot l^{-1}$, pH 7.9), 74.46 mg EDTA (2 $nmol \cdot l^{-1}$), 75.56 mg KCl (10 $nmol \cdot l^{-1}$), 14.28 mg $MgCl_2$ (1.5 $nmol \cdot l^{-1}$) dissolved in 80 ml of dH_2O, pH adjusted to 7.9 with HCl and added dH_2O to 100 ml, before using it was added 2 $mmol \cdot l^{-1}$ PMSF (20 µl for 1 ml of hypotonic buffer) and protease inhibitors (40 µl for 1 ml of hypotonic buffer)

- Stacking polyacrylamide gel: 670 µl 30% acrylamide/bis-acrylamide, 2.975 ml dH_2O, 1.25 ml stacking gel buffer, 50 µl 10% (w/v) SDS, 50 µl 10% (w/v) APS, 5 µl TEMED

- TBST buffer: 100 ml 1× TBS buffer, 900 ml dH_2O, 1 ml 0.1% Tween 20

4.3 Drugs

- Laulimalide (provided by Dr. Rob Keyzers, School of Chemical and Physical Sciences, Victoria University of Wellington, Wellington, New Zealand)
- Paclitaxel (Ebewe)

4.4 List of equipment

- –80 °C freezer
- 6-well and 96-well plates (TPP Techno Plastic Products AG)

- o Automatic pipetting filler Pipetus® (Hirschmann™)
- o Axio Observer D1 Fluorescent microscope (Carl Zeiss)
- o Benchtop Centrifuge 5810R (Eppendorf centrifuge)
- o BTD Dry Block Heating System (Grant Instruments™)
- o Combined Centrifuge/Vortex mixer Multi-Spin PCV-6000 (Grant-Bio)
- o EnSpire Multimode Plate Reader 2300-001M (Perkin Elmer)
- o Eppendorf pipettes (0.5–1000 µl)
- o FastGene Mini Centrifuge (Nippon Genetics)
- o Heracell™ VIOS incubator (ThermoFisher Scientific™)
- o Laminar flowbox MSC-Advantage™ Class II Biological Safety Cabinet (ThermoFisher Scientific™)
- o Molecular Imager® Gel Doc™ XR System (Bio-Rad)
- o Olympus IX51 Inverted Phase Contrast Fluorescence Microscope (Olympus)
- o pH meter (Denver Instrument)
- o PowerPac™ HC Power Supply (Bio-Rad)
- o Rotina 420R Centrifuge (Hettich Zentrifugen)
- o Trans-Blot Turbo RTA Transfer Kit, PVDF (Bio-Rad, cat. No. 170-4272)
- o Trans-Blot Turbo Transfer System (Bio-Rad, cat. No. 1704150)
- o ViCell™ XR Cell Viability Analyzer (Beckman Coulter)
- o Vortex V-1 Plus (Biosan)

4.5 Biological material

Two different human carcinoma cell lines, colorectal cancer HCT116 cells, and alveolar epithelial adenocarcinoma A549 cells, were purchased from ATCC (Manassas, VA, USA). HCT116 cells were maintained in McCoy's 5A media with L-glutamine (Lonza, cat. No. 12-688F) supplemented with 10% FBS and 1× Penicillin-Streptomycin, whereas A549 cells were cultured in Ham's F-12 medium (Kaighn's modification) with L-glutamine (Sigma Aldrich, cat. No. N3520) supplemented with 10% FBS, 20% $NaHCO_3$ and 1× Penicillin-Streptomycin. Cells were cultured under normoxic conditions in ambient air, 5% CO_2 incubator at 37 °C. For hypoxic induction, cells were subjected to 1% O_2.

4.6   Experimental and evaluation procedures

4.6.1 Cell cultivation

Cell lines were incubated in T75 cell culture plastic flasks with an appropriate medium. Cells were passaged regularly 2–3 times a week and used for the experiment when they reached 80% confluency. This measure was estimated by observing cells under a microscope. Old media was discarded into a waste container and cells were washed twice with 10 ml 1× PBS. Thereafter, cells were washed with 1 ml of TrypLE and incubated in thermostat for 2 minutes at 37 °C. After incubation, the flask was observed under a microscope to see if the cells have had detached, if not the flask was gently tapped to facilitate cell detachment. Detached cells were collected in 10 ml of complete media by rinsing the flask with the medium. The cell suspension was transferred to a 15-ml Falcon tube with colonial bottom and centrifuged at 300× g for 5 minutes. The supernatant was discarded, and the cell pellet was resuspended in 5 ml of media. Next, 0.5 ml of suspension was used to determine cell density and percentage of viability using ViCell Cell Counter. According to cell density, the cells were seeded in the flask with 15 ml of media for propagation.

4.6.2 Cell viability assay

Cell viability was determined by a 3-[4,5-dimethylthiazol-2-yl]-2,5-diphenyl tetrazolium bromide (MTT) assay, which is a colorimetric method based on the reduction of the MTT dye to violet formazan crystals by mitochondrial succinate dehydrogenase in living cells. Cells were seeded in a 96-well plate at a density of 10 000 cells/ml (for HCT116 cell line) or 50 000 cells/ml (for A549 cell line) and cultured overnight in a standard CO_2 incubator or an incubator with hypoxic conditions. The next day cells were treated with drugs for 72 hours. Drugs were added to the first set of triplicate wells and serially diluted. Each plate contained appropriate 'no drug controls'. After 72 hours, 10 μl of MTT solution was added to each well, and the culture plate was incubated for 2 hours in a 37 °C incubator wrapped in an aluminium foil. Next, 100 μl of SDS was added in each well and the plate was left until the next day in the incubator. The absorbance was measured the next day in an EnSpire Plate Reader at 570 nm and the IC_{50} values of drugs were determined from their respective dose-response curves using GraphPad Prism (GraphPad Software, San Diego, CA).

4.6.3 *In vitro* tubulin polymerization assay

Cells were plated in 6-well plates at a density of 250 000 cells/ml (HCT116) and 500 000 cells/ml (A549). The next day the medium was removed, and cells were treated with LAU and PTX for 24 hours. Used LAU concentrations were 0, 5, 25, 50, 200, 1 000 nmol·l^{-1}, whereas PTX were used at 10× lower concentrations – 0.5, 2.5, 5, 20, 100 nmol·l^{-1}. Cells were imaged before and after treatment using a microscope. Following treatment, cells were washed twice with 1× PBS buffer and lysed with 100 µl of hypotonic buffer (supplemented with 2 mmol·l^{-1} PMSF and protease inhibitors) for 5 minutes at 37 °C. The lysates were then transferred to a 1.5ml Eppendorf tube. The well was re-rinsed by another 100 µl of the hypotonic buffer to extract all remaining cells. The samples were vortexed briefly and centrifuged at 14 000 rpm for 10 minutes at room temperature. The supernatant (soluble) was collected and transferred into a new Eppendorf tube and stored as the cytosolic fraction. The remaining pellet (insoluble) was resuspended in 200 µl of the hypotonic buffer and stored as the cytoskeletal fractions.

4.6.4 Gel electrophoresis and western blot

The cytosolic and cytoskeletal tubulin fractions were mixed with 5× SDS-PAGE sample buffer containing 10% β-Mercaptoethanol and boiled at 95 °C for 5 minutes. An equal volume of samples was loaded per well and electrophoresed by 12% SDS-PAGE in 1×Tris/Glycine/SDS running buffer at 120 V for 90 minutes. The first lane of the gel was loaded with Spectra Multicolour Protein Ladder and run alongside with protein samples.

Following electrophoresis, proteins were transferred into a PVDF membrane using in 1× transfer buffer (20 ml of ethanol, 20 ml of Trans-Blot Turbo 5× Transfer Buffer and 60 ml of distilled water). To prevent non-specific antigen-antibody binding, the membranes were blocked in 5% bovine serum albumin (1 g of BSA was dissolved in 1× TBS with 0.1% Tween-20 solution) for 1 hour, occasionally overnight at 4 °C. Following blocking, membranes were washed once with TBST for 5 minutes and then incubated with primary antibody α-Tubulin (1 : 6 000) for 45 minutes at room temperature. The primary antibody binds with a high affinity to specific epitopes, tubulin in this case. Following incubation with the primary antibody, membranes were washed 3 times (5 minutes each) with TBST and then re-incubated with secondary antibody (Alexa Fluor 488, 1 : 2 000) for 1 hour in dark. After incubation, the immunoblots were

visualized using a Molecular Imager® Gel Doc™ XR System. Using the ImageJ program was calculated the intensity of individual blots (the percentage of soluble tubulin and polymerized tubulin).

4.6.5 Alamar blue assay

Cells were seeded in 96-well plates at a density of 10 000 cells/ml (HCT116) and 50 000 cells/ml (A549) in 100 µl of media. Plates were incubated overnight in standard or hypoxic incubators. The next day the medium was removed, and cells were treated with LAU and PTX for 24 hours. LAU concentrations used were 0, 5, 25, 50, 200, 1 000 nmol·l^{-1}, whereas PTX was used at 10× lower concentrations. On the day of the cell viability experiment, cell viability reagent was brought to room temperature. Ten µl of the drug was removed from each well and the same volume of cell viability reagent was added. Plates were incubated for 2 hours in standard incubators and the absorbance was read using an EnSpire Plate Reader at 570 nm.

4.6.6 Image processing, data analysis, and final compilation

For editing and exporting images was used:
- o Fluorescent microscope (Carl Zeiss Axio Observer D1)
- o ImageJ ver. 1.52a (available at: https://imagej.nih.gov/ij/)
- o Microsoft PowerPoint ver. 16.37
- o ACD/Chemsketch (Freeware) ver. 12.01
- o Inkscape ver. 0.92

For statistical analysis and graphing data was used:
- o GraphPad Prism 8
- o Microsoft Excel ver. 16.37

5 RESULTS

5.1 Laulimalide sensitivity in normoxic and hypoxic conditions

5.1.1 Cytotoxicity of Laulimalide

The effects of microtubule-stabilizing drug LAU under normoxic and hypoxic conditions were compared with those of PTX in human cancer cell lines HCT116 and A549. The drug sensitivity was assessed by the cell viability assay as described in Chapter 4.5.2. To determine if hypoxic conditions affect LAU cytotoxicity, parental cells were incubated in hypoxic conditions prior to and after exposing cells to the cytotoxic drug. The starting concentration of LAU was 500 nmol·l^{-1} (3-fold dilution; 10 data points) for HCT116 cells and 1 μmol·l^{-1} (4-fold dilution; 10 data points) for A549 cells for LAU and PTX. Treatment of both cancer cell lines with LAU and PTX lasted for 72 hours under appropriate conditions. The experiment was performed four times in triplicates for each cell line and drug.

As shown in Table 5.1, the maximal half inhibitory concentration of LAU is greater than PTX in both cell lines irrespective of whether cultured under normoxia or hypoxia, whereas LAU has similar low nanomolar potency as PTX. Hypoxic cells are more sensitive either to LAU and PTX, this may correlate with their higher sensitivity and lower cell viability. Although hypoxia did not affect the cytotoxicity of LAU in HCT116 significantly, the difference between A549 cells was less sensitive to LAU than HCT116 cells as shown in Figure 5.1 and Table 5.1. For A549 cells, a higher concentration of LAU had to be used to inhibit their viability. The IC$_{50}$ values of LAU and PTX are higher in A549 cells than in HCT116 cells as can be seen in Table 5.1. The cytotoxic efficacy of PTX is greater in both cell lines whether incubated in hypoxia or normoxia, which was expected due to the high toxic properties of PTX. HCT116 cells are more sensitive to both used drugs which can be seen from the low IC$_{50}$ values, for normoxic cells it was 0.81 ± 0.57 nmol·l^{-1} and hypoxic 0.62 ± 0.17 nmol·l^{-1}. In contrast to HCT116 cells, A549 are less sensitive to LAU, the IC$_{50}$ value in normoxic A549 cells is 5.46 ± 1.65 nmol·l^{-1} and in hypoxic cells 4.90 ± 1.29 nmol·l^{-1}.

According to IC50 values, hypoxic A549 cells are more sensitive to LAU than normoxic cells and a similar result is seen in HCT116 cells.

Table 5.1 Averaged IC_{50} concentrations ($nmol \cdot l^{-1}$) of LAU and PTX in HCT116 and A549 cells in normoxia and hypoxia. Data are mean $\pm$ SEM, n = 4

|		**HCT116**	**A549**
LAU	Normoxia	0.81 ± 0.57	5.46 ± 1.65
	Hypoxia	0.62 ± 0.17	4.90 ± 1.29
PTX	Normoxia	0.30 ± 0.25	2.37 ± 1.27
	Hypoxia	0.21 ± 0.15	2.10 ± 0.54
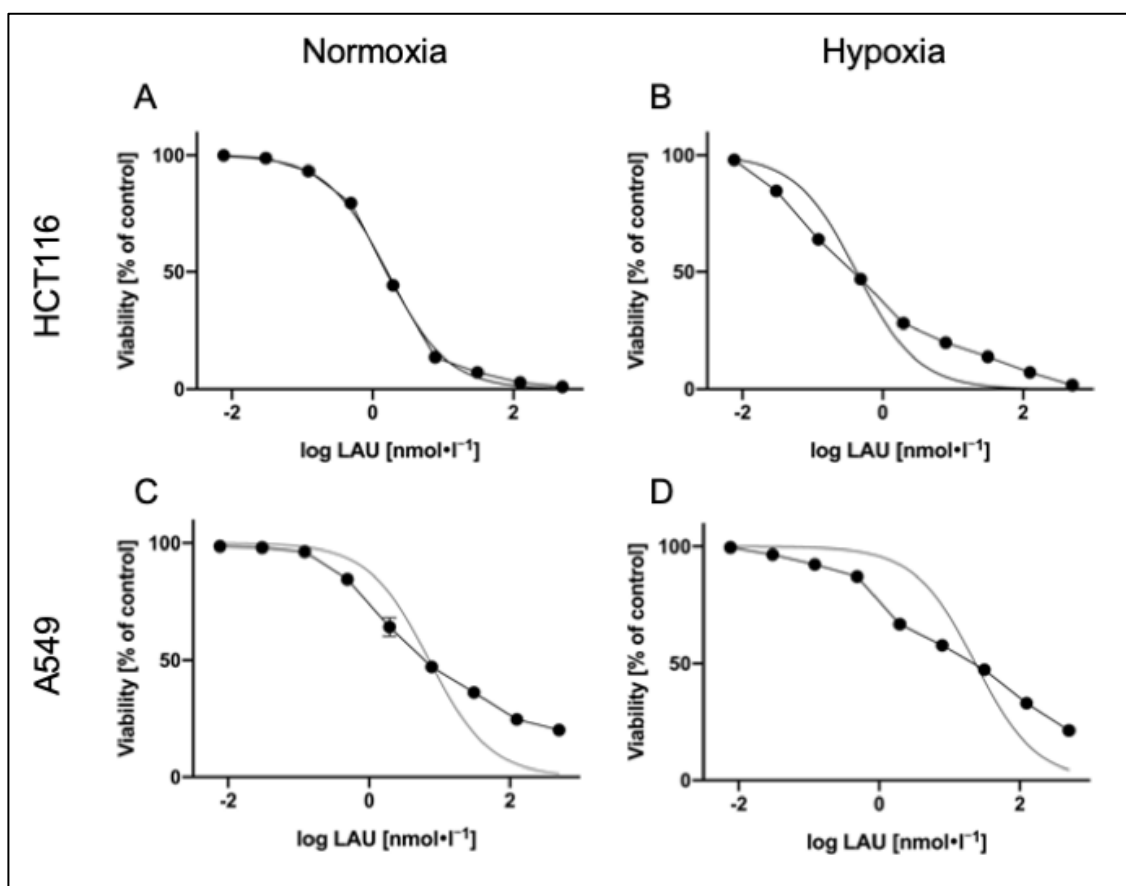
Figure 5.1 Representative dose-response curves demonstrating effects of LAU on cell viability of HCT116 (A, B) and A549 (C, D) under normoxic (A, C) and hypoxic (B, D) conditions.

5.1.2 Cell proliferation

Both cell lines, HCT116 and A549, were treated for 24 h with LAU at 5, 25, 50, 200, 1000 $nmol \cdot l^{-1}$ or PTX at 0.5, 2.5, 5, 20, 100 $nmol \cdot l^{-1}$ concentration as was described in Chapter 4.5.6. Cell proliferation was analysed by Alamar Blue assay and the absorbances were measured after 2 hours and 24 hours of incubation.

The results show similar effects on cell proliferation by using LAU or PTX. The reduced growth rate correlated with the increased concentration of drugs. The cell number of normoxic HCT116 dropped by approximately 50 % at the highest drug concentration (LAU – 1 $\mu mol \cdot l^{-1}$) after 2 hours of incubation with Alamar blue. After 24 hours, cell proliferation was 100 %, indicating the proliferation was renewed, probably due to the new cell population. The proliferation of hypoxic HCT116 cells was approximately 40 %, at the highest tested drug concentration, but the inhibitory effects were delayed, the inhibition of cell proliferation cames after 24 hours. However, A549 cells were less susceptible to LAU and PTX, and the percentage of proliferating cells was higher than of HCT116, for both, normoxic and hypoxic cells it was around 60–70 %. In Figure 5.2, it can be observed that the proliferation of A549 cells is around 60 %, but HCT116 is below 60 % whether the cells are hypoxia-conditioned or not. HCT116 cells respond to cell proliferation inhibition by LAU better than A549 cells. After 24 hours, the values of cell proliferation of normoxic cells have grown to almost 100 %. Thus, the ability to proliferate was restored, although the proliferation of HCT116 hypoxic cells was inhibited after 24 hours, A549 cells react to treatment even after 2 hours.
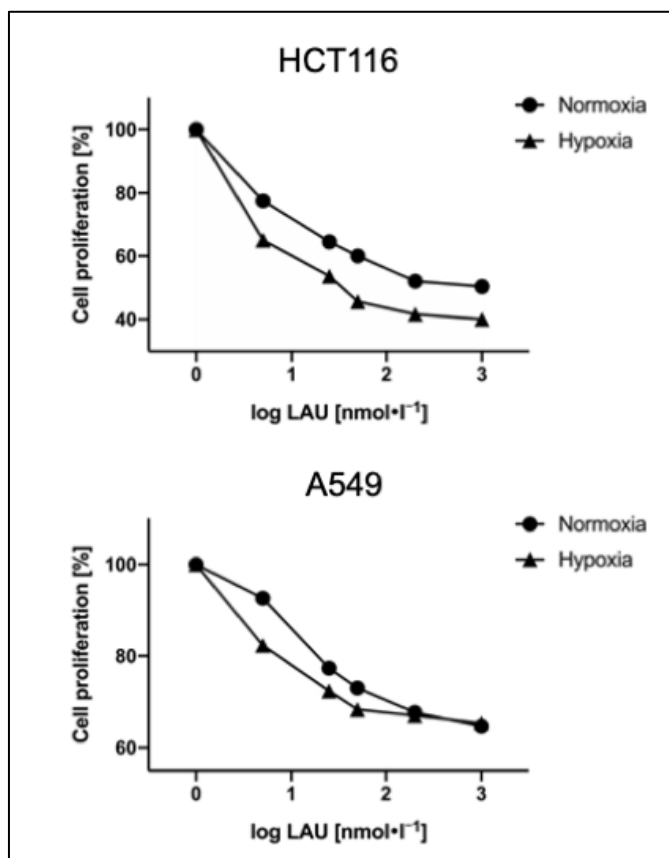
Figure 5.2 A graphic representation of concentration-response curves which demonstrates cell proliferation of HCT116 (normoxia after 2 hours and hypoxia after 24 hours of incubation with Alamar blue) and A549 (after 2 hours of incubation with Alamar blue) in relation to increasing drug concentration. The experiment was performed in triplicate.

5.1.3 Microscopy and imaging

Cells were imaged before and after 24-hour treatment with 1 μmol·l⁻¹ LAU or 100 nmol·l⁻¹ PTX using a phase-contrast microscope to observe morphological changes. Figures 5.3 (HCT116) and 5.4 (A549) describe a typical morphology of dead cells – spherical and rounded cells with a dark centre and a brighter exterior rim. Additionally, a significant cell loss can be observed under hypoxic conditions after the treatment of HCT116 with both drugs. The morphology of untreated normoxic and hypoxic cells appear similar (Figure 5.3).
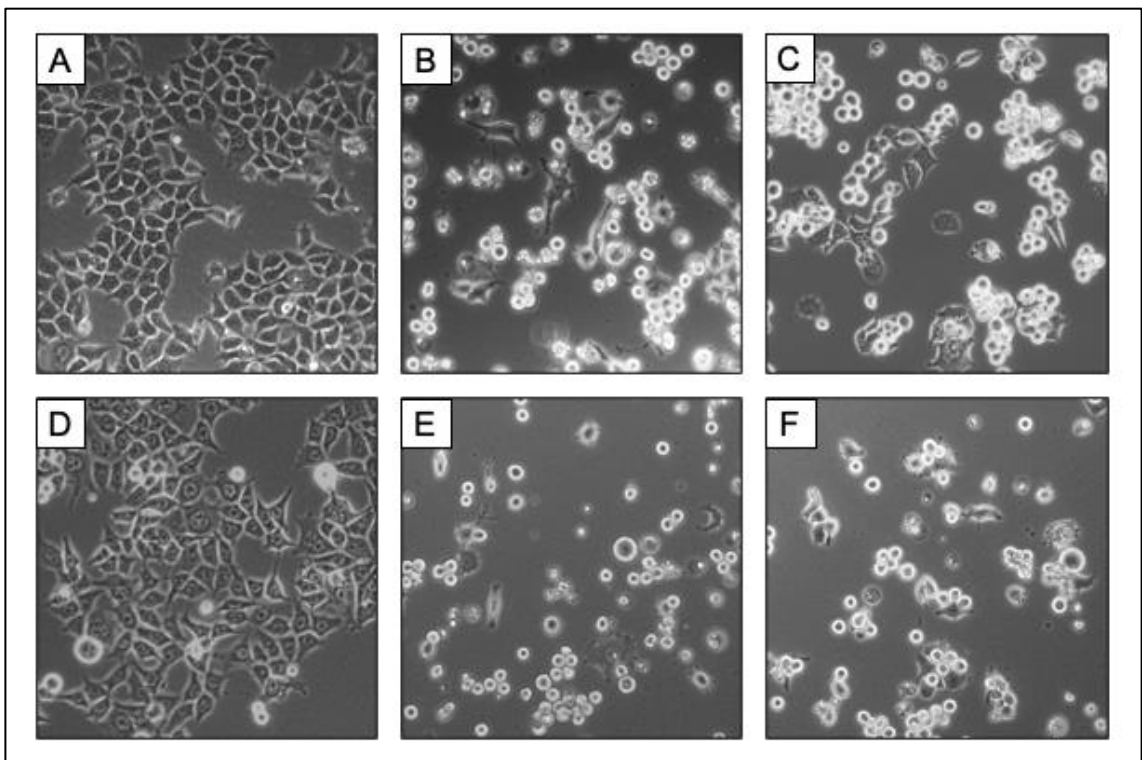
Figure 5.3 Morphological changes in HCT116 cells incubated in normoxia (A, B, C) and hypoxia (D, E, F). Phase-contrast photomicrographs are presented of HCT116 cells untreated (A – normoxia, D – hypoxia) and treated with 1 μmol·l⁻¹ LAU (B – normoxia, E – hypoxia) or 100 nmol·l⁻¹ PTX (C – normoxia, F – hypoxia) for 24 hours. Objective: 10×. Magnification 100×

It can be seen in Figure 5.4, normoxic cells (A) are wider and less elongated than hypoxic cells (D). This suggests the induction of a mesenchymal cell type. Compared to untreated, rounding and lifting of cells are evident after treatment with both the drugs under the two culture conditions. A decrease in cell number is evident after treatment with PTX, which is known to be more cytotoxic than LAU.
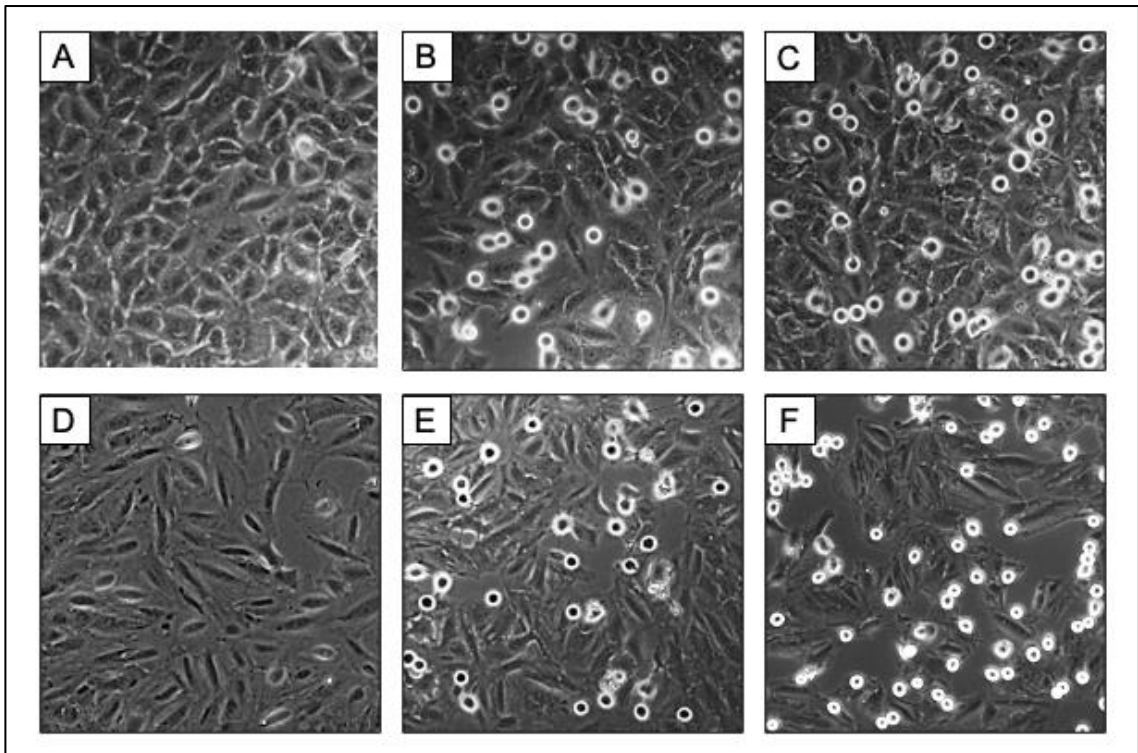

Figure 5.4 Morphological changes in A549 cells incubated in normoxia (A, B, C) and hypoxia (D, E, F). Phase-contrast photomicrographs are presented of A549 cells untreated (A – normoxia, D – hypoxia) or treated with 1 μmol·l^{-1} LAU (B – normoxia, E – hypoxia) and 100 nmol·l^{-1} PTX (C – normoxia, F – hypoxia) for 24 hours. Objective: 10×, Magnification 100×

5.2 Microtubule stabilizing effects of laulimalide

To determine the stabilizing effects of LAU on microtubules, tubulin *in vitro* polymerization assay was performed as described in Chapter 4.5.3. Cells were incubated in normoxia or hypoxia and were treated with either LAU or PTX for 24 hours.

It is assumed that with an increased concentration of microtubule-stabilizing drugs, there will be a decrease in soluble tubulin and an increase in polymerized tubulin. This can be observed in cells incubated in normoxia (Figure 5.5 and 5.6), where the concentration of soluble tubulin decreases with increasing concentration of either LAU (A) or PTX (B), whereas in cells treated with PTX the effect is not that distinct. In hypoxic HCT116 cells treated with LAU, an increasing concentration of polymerized tubulin as in normoxic cells can be observed, which means that LAU encouraged tubulin clustering even in hypoxic cells. However, in A549 hypoxic cells treated with either LAU or PTX and PTX-treated hypoxic HCT116 cells, low concentrations of soluble tubulin can be observed. Also, in untreated cells, the concentration of polymerized tubulin is higher than that observed in untreated normoxic cells. This is possibly an adaptive mechanism for hypoxia, which supports cell survival even in harsh conditions. Although the concentration of polymerized tubulin is higher in hypoxic cells, this can be influenced by used drugs.
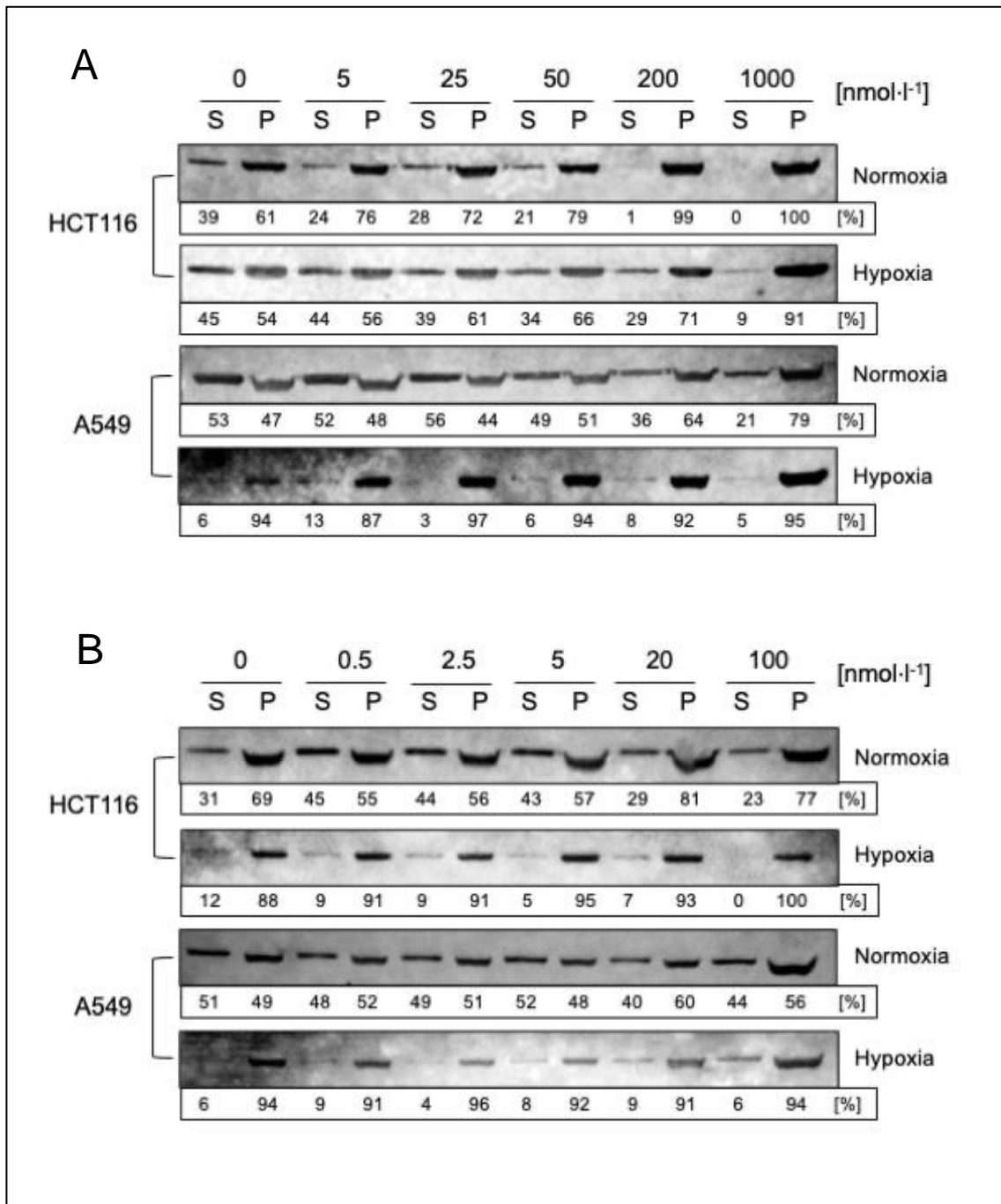
Figure 5.5 Representative immunoblots of α-Tubulin after electrophoresis of soluble (S) and polymerized tubulin (P) fractions of HCT116 and A549 cells incubated either in normoxia or hypoxia, following 24 hours of exposure to LAU (A) or PTX (B). The numbers below the blots are the percentage of soluble and polymerized tubulin. Tubulin heterodimer molecules have a molecular size of 55 kDa (Sigma-Aldrich). The experiments were repeated at least two times.

6 DISCUSSION

MSAs are extensively used in anticancer treatment. Since hypoxia has been shown to limit the efficacy of MTAs such as PTX, it is important to find alternative MSAs that can overcome hypoxia-induced resistance mechanisms (Das *et al.*, 2015). In the last few years, there has been a growing interest in MSAs such as PLA (Řehulka *et al*., 2017) and LAU that bind to non-taxane sites but have PTX-like effects to overcome resistance to taxane site drugs. Many studies are performed in normoxic cell lines. The focus of this thesis was to determine the cytotoxic effects of LAU in hypoxic HCT116 and A549 cell lines.

Cells were treated for 72 hours under appropriate conditions, and cell viability assays were performed to determine IC_{50} values of LAU and PTX in normoxic and hypoxic cancer cell lines. Compared to PTX, the IC_{50} values of LAU were higher (see Figure 5.1 and Table 5.1), which is expected because PTX is known to be more toxic than other MSAs such as PLA that binds to the same site as LAU. Both LAU and PTX showed similar low nanomolar potencies for cell growth inhibition as confirmed in Liu *et al*. work (2007). PTX is a potent drug but its cytotoxicity is often limited by hypoxia due to changes in MT stability (Zeng *et al*., 2007). The cell viability data show that HCT116 cell exposure to hypoxia does not have a significant effect on the cytotoxic properties of LAU. Although A549 cells have a higher susceptibility to PTX than to LAU, hypoxic cells are more sensitive to LAU than normoxic cells. Thus, data has shown that LAU retains cytotoxic effects even in hypoxic cancer cell lines.

Cell proliferation assay (Figure 5.2) show that in HCT116 the cell growth rate decreases with drug concentration, in normoxia dropped to 50 % after 2 hours of incubation with Alamar blue reagent (24 hours of treatment) at the highest LAU concentration, whereas in hypoxic cells, the proliferation was about 40 % but after 24 hours of incubation with Alamar blue reagent (48 hours of treatment). After 24 hours of incubation with Alamar blue reagent, normoxic cells showed 100% cell proliferation. Hypoxic A549 cells showed similar cell growth as normoxic cells (ca. 70 %) after 2 hours of incubation, but after 24 hours the cell proliferation grows up to 100 %. The results of this assay are therefore confusing and suggest not so effective inhibition of cell proliferation. Further, the morphological changes caused by hypoxic conditions were more prominent in A549 cells than HCT116. The A549 cells showed an elongated,

spindle-shaped morphology under hypoxia suggesting a change into mesenchymal cell type.

The *in vitro* tubulin polymerization assay results show that in normoxia the soluble tubulin polymerizes with increasing concentration of LAU. Our data show that hypoxia affects the concentration of soluble tubulin in treated or untreated in both used cancer cell lines. Hypoxia has its own mechanism that supports MT polymerization for cell survival in hypoxic conditions. Cells adapt themselves to this level of MT stabilization in hypoxia, so it could be observed a high percentage of polymerized tubulin even in untreated cells. Anoxic conditions ($< 2\%$ O_2) decrease MT polymerization, while physiological hypoxia (3% O_2) stabilizes MTs by its own mechanisms to enable cell survival under the harsh conditions and thereby supports tumour growth (Yoon *et al*., 2005; Parker *et al*., 2014). Further, hypoxia affects the expression of MAPs which is associated with MTA resistance (Xie *et al*., 2015). Our data show that hypoxia affects the concentration of soluble tubulin in treated or untreated in both used cancer cell lines. However, the concentration of polymerized tubulin was supported by LAU treatment. In PTX-treated hypoxic cells, the concentration of polymerized tubulin is similar to that in untreated cells indicating that hypoxia affects PTX-mediated stabilization of MTs. Thus, the properties promoting tubulin polymerization was confirmed in cells treated with LAU.

Due to a different binding site, LAU is expected to have better anti-tumour effects in hypoxic cells. LAU initiates tubulin polymerization, as it can be observed in our study (Figure 5.5), and others (Bajaj *et al*., 2013; Mooberry *et al*., 1999). Notably, the concentration of PTX used in the treatment of used cell lines was 10 times lower than the concentration of LAU and a comparison of effects of LAU and PTX show that PTX is still more potent than LAU (Moobery *et al*., 1999) as it could be seen in Table 5.1. Studies have shown that LAU is a poor substrate of Pg-P cellular drug efflux pump and blocks mitosis (Mooberry *et al*., 1999; Liu *et al*., 2007), by inducing the formation of microtubule bundles and abnormal mitotic spindles, leading to apoptosis (Moobery *et al*., 2004). On the other hand, *in vivo* studies have shown that LAU does not inhibit tumour growth significantly unlike PTX and the effects of LAU are highly reversible (Liu *et al*., 2007). Although LAU has promising cytotoxic and MT stabilizing properties, it is limited by its toxicity (Liu *et al*., 2007). This has resulted in studies to find LAU analogues with lower toxicity and better or similar efficacy to PTX (Churchill *et al*., 2015).

7 CONCLUSION

This thesis was focused on determining cytotoxic and microtubule-stabilizing effects of LAU in hypoxic HCT116 and A549 cell lines. As LAU binds to a different site on tubulin heterodimer than PTX, it is assumed that LAU could have similar effects as PTX, but not affected by hypoxia. Hypoxia is a complex multifactorial issue in solid tumours and cannot be recapitulated entirely in cellular studies.

All data of experiments using LAU were compared with PTX. It was found that LAU has similar low nanomolar potencies as PTX and the susceptibility of the two cancer cell lines to LAU was not affected by hypoxia. The IC_{50} value of LAU in hypoxic HCT116 was 0.62 ± 0.17 nmol·l^{-1}, and in A549 cells was 4.90 ± 1.29 nmol·l^{-1}. It was also found that A549 cells are more resistant to PTX. Although hypoxia does not have significant effects on cytotoxic properties of LAU, inhibition of proliferation of hypoxic HCT116 was delayed than of normoxic cells and in A549 was inhibition the same in normoxic and hypoxic cells. After 24 hours was cell proliferation renewed in both cell lines except for hypoxic HCT116 cells.

It was confirmed, that LAU stimulates tubulin polymerization in normoxic, but also hypoxic cancer cell lines. Hypoxia on its own increased polymerized tubulin, however, LAU induced further polymerization of tubulin in treated hypoxic cells, the increasing percentage of polymerized tubulin corresponded to the increasing LAU concentration.

LAU is known to have off-target toxicity and low tumour inhibitory effect limiting its current use for cancer treatment. Thus, there is a growing interest in LAU analogues with similar cytotoxicity but improved properties. These findings show promising effects of LAU under hypoxic conditions and will encourage further development of LAU analogues.

8 REFERENCES

Alberts, Bruce. 2002. *Molecular Biology Of The Cell*. 4th ed. New York: Garland Science.

Alberts, Bruce, Dennis Bray, Julian Lewis, Martin Raff, Keith Roberts, and James Dewey Watson. 1994. *Molecular Biology Of The Cell*. 3rd Ed. New York: Garland Publishing.

Altmann, Karl-Heinz, Guido Bold, Giorgio Caravatti, Nicole End, Andreas Flörsheimer, Vito Guagnano, Terence O'Reilly, and Markus Wartmann. 2000. "Epothilones And Their Analogs - Potential New Weapons In The Fight Against Cancer". *Chimia: International Journal For Chemistry* 54 (11): 612–621.

Amos, Linda A. 2011. "What Tubulin Drugs Tell Us About Microtubule Structure And Dynamics" 22 (9): 916-926.

Arnal, Isabelle, and Richard H. Wade. 1995. "How Does Taxol Stabilize Microtubules?". *Current Biology* 5 (8): 900-908.

Avila, Jesús. 1992. "Microtubule Functions". *Life Sciences* 50 (5): 327-334.

Bajaj, Megha, Martin Srayko, and Yanchang Wang. 2013. "Laulimalide Induces Dose-Dependent Modulation Of Microtubule Behaviour In The C. Elegans Embryo". *Plos One* 8

Bornens, M. 2012. "The Centrosome In Cells And Organisms". *Science* 335 (6067): 422-426.

Cooper, Geoffrey M. 2000. *The Cell : A Molecular Approach*. 2nd ed.. Sunderland (MA): Sinauer Associates.

Das, Viswanath, Jana Štěpánková, Marián Hajdúch, and John H. Miller. 2015. "Role Of Tumor Hypoxia In Acquisition Of Resistance To Microtubule-Stabilizing Drugs". *Biochimica Et Biophysica Acta (Bba) - Reviews On Cancer* 1855 (2): 172-182.

Gertsch, Jürg, Sarah Meier, Martin Müller, and Karl-Heinz Altmann. 2009. "Differential Effects Of Natural Product Microtubule Stabilizers On Microtubule Assembly: Single Agent And Combination Studies With Taxol, Epothilone B, And Discodermolide". *Chembiochem* 10 (1): 166-175.

Goodin, Susan, Michael P. Kane, and Eric H. Rubin. 2004. "Epothilones: Mechanism Of Action And Biologic Activity". *Journal Of Clinical Oncology* 22 (10): 2015-2025.

Höckel, M., and P. Vaupel. 2001. "Tumor Hypoxia: Definitions And Current Clinical, Biologic, And Molecular Aspects". *Jnci Journal Of The National Cancer Institute* 93 (4): 266-276.

Churchill, Cassandra D.M., Mariusz Klobukowski, and Jack A. Tuszynski. 2015. "Analysis Of The Binding Mode Of Laulimalide To Microtubules: Establishing A Laulimalide–Tubulin Pharmacophore". *Journal Of Biomolecular Structure And Dynamics* 34 (7): 1455-1469.

Jordan, Mary Ann, and Leslie Wilson. 2004. "Microtubules As A Target For Anticancer Drugs". *Nature Reviews Cancer* 4 (4): 253-265.

Kanakkanthara, A., P. T. Northcote, and J. H. Miller. 2012. " Ii-Tubulin And Iii-Tubulin Mediate Sensitivity To Peloruside A And Laulimalide, But Not Paclitaxel Or Vinblastine, In Human Ovarian Carcinoma Cells". *Molecular Cancer Therapeutics* 11 (2): 393-404.

Kanakkanthara, Arun, Peter T. Northcote, and John H. Miller. 2016. "Peloruside A: A Lead Non-Taxoid-Site Microtubule-Stabilizing Agent With Potential Activity Against Cancer, Neurodegeneration, And Autoimmune Disease". *Natural Product Reports* 33 (4): 549-561.

Kavallaris, Maria. 2010. "Microtubules And Resistance To Tubulin-Binding Agents". *Nature Reviews Cancer* 10 (3): 194-204.

Lambert, Anne-Marie. 1993. "Microtubule-Organizing Centers In Higher Plants". *Current Opinion In Cell Biology* 5 (1): 116-122.

Liu, J, MJ Towle, and H Cheng. 2007. "In Vitro And In Vivo Anticancer Activities Of Synthetic (-)-Laulimalide, A Marine Natural Product Microtubule Stabilizing Agent.". *Anticancer Research* 2007 (27(3B): 1509-1518.

M. Bollag, Daniel, Patricia A. McQueney, Jian Zhu, Otto Hensens, Lawrence Koupal, Jerrold Liesch, Michael Goetz, Elias Lazarides, and Catherine M. Woods. 1995. "Epothilones, A New Class Of Microtubule-Stabilizing Agents With A Taxol-Like Mechanism Of Action". *Cancer Research* 1995 (Volume 55): 2325-2333.

Mitchison, Tim, and Marc Kirschner. 1984. "Dynamic Instability Of Microtubule Growth". *Nature* 312 (5991): 237-242.

Mooberry, S. L., D. A. Randall-Hlubek, R. M. Leal, S. G. Hegde, R. D. Hubbard, L. Zhang, and P. A. Wender. 2004. "Microtubule-Stabilizing Agents Based On Designed Laulimalide Analogues". *Proceedings Of The National Academy Of Sciences* 101 (23): 8803-8808.

Mooberry, Susan L., Georgia Tien, Anne H. Hernandez, Anuchit Plubrukarn, and Bradley S. Davidson. 1999. "Laulimalide And Isolaulimalide, New Paclitaxel-Like Microtubule-Stabilizing Agents". *Cancer Research* 1999 (59): 653–660.

Nakazawa, Michael S., Brian Keith, and M. Celeste Simon. 2016. "Oxygen Availability And Metabolic Adaptations". *Nature Reviews Cancer* 16 (10): 663-673.

Nogales, Eva. 2001. "Structural Insights Into Microtubule Function". *Annual Review Of Biophysics And Biomolecular Structure* 30 (1): 397-420.

Nogales, Eva, Sharon G. Wolf, and Kenneth H. Downing. 1998. "Structure Of The Aβ Tubulin Dimer By Electron Crystallography". *Nature* 391 (6663): 199-203.

Parker, Amelia L., Maria Kavallaris, and Joshua A. McCarroll. 2014. "Microtubules And Their Role In Cellular Stress In Cancer". *Frontiers In Oncology* 4 (June).

Prota, Andrea E., Katja Bargsten, Peter T. Northcote, May Marsh, Karl-Heinz Altmann, and John H. Miller. 2014. "Structural Basis Of Microtubule Stabilization By Laulimalide And Peloruside A". *Angewandte Chemie International Edition* 53 (6).

Pryor, Donald E., Aurora O'Brate, Geoffrey Bilcer, J. Fernando Díaz, Yuefang Wang, Yong Wang, Mikio Kabaki, *et al*. 2002. "The Microtubule Stabilizing Agent Laulimalide Does Not Bind In The Taxoid Site, Kills Cells Resistant To Paclitaxel And Epothilones, And May Not Require Its Epoxide Moiety For Activity †". *Biochemistry* 41 (29): 9109-9115.

Řehulka, Jiří, Narendran Annadurai, Ivo Frydrych, Pawel Znojek, Petr Džubák, Peter Northcote, John H. Miller, Marián Hajdúch, and Viswanath Das. 2017. "Cellular Effects Of The Microtubule-Targeting Agent Peloruside A In Hypoxia-Conditioned Colorectal Carcinoma Cells". *Biochimica Et Biophysica Acta (Bba) - General Subjects* 1861 (7): 1833-1843.

Schek, Henry T., Melissa K. Gardner, Jun Cheng, David J. Odde, and Alan J. Hunt. 2007. "Microtubule Assembly Dynamics At The Nanoscale". *Current Biology* 17 (17): 1445-1455.

Schiff, Peter B., Horwitz Suzan B. and Fant J. 1979. "Promotion Of Microtubule Assembly In Vitro By Taxol". *Nature* 277 (5698): 665–667.

Takáčová, Martina, and Silvia Pastoreková. 2015. "Tumour Hypoxia – Molecular Mechanisms And Clinical Relevance". *Klinicka Onkologie* 28 (3): 183-190.

Ur-Rahman, Atta, and Khurshid Zaman. 2018. *Topics In Anti-Cancer Research*. 7 ed.. Sharjah, UAE: Bentham Science.

Vaughn, Kevin. 2013. *Immunocytochemistry Of Plant Cells*. 1st ed.. Netherlands: Springer Netherlands.

Vaupel, Peter, Oliver Thews, and Hoeckel. 2001. "Treatment Resistance Of Solid Tumors: Role Of Hypoxia And Anemia". *Medical Oncology* 18 (4): 243–259.

Xie, Songbo, Angela Ogden, Ritu Aneja, and Jun Zhou. 2016. "Microtubule-Binding Proteins As Promising Biomarkers Of Paclitaxel Sensitivity In Cancer Chemotherapy". *Medicinal Research Reviews* 36 (2): 300-312.

Yoon, Sang-Oh, Sejeong Shin, and Arthur M. Mercurio. 2005. "Hypoxia Stimulates Carcinoma Invasion By Stabilizing Microtubules And Promoting The Rab11 Trafficking Of The A6B4 Integrin". *Cancer Research* 65 (7): 2761-2769.

Zeng, Lihua, Shinae Kizaka-Kondoh, Satoshi Itasaka, Xuejun Xie, Masahiro Inoue, Keiji Tanimoto, Keiko Shibuya, and Masahiro Hiraoka. 2007. "Hypoxia Inducible Factor-1 Influences Sensitivity To Paclitaxel Of Human Lung Cancer Cell Lines Under Normoxic Conditions". *Cancer Science* 98 (9): 1394-1401.